

## A Framework for Indoor Localization Using the Magnetic Field

Kok, M.; Viset, F.M.; Osman, M.E.A.

**DOI**

[10.1109/MDM55031.2022.00086](https://doi.org/10.1109/MDM55031.2022.00086)

**Publication date**

2022

**Document Version**

Final published version

**Published in**

Proceedings of the 23rd IEEE International Conference on Mobile Data Management (MDM 2022)

**Citation (APA)**

Kok, M., Viset, F. M., & Osman, M. E. A. (2022). A Framework for Indoor Localization Using the Magnetic Field. In *Proceedings of the 23rd IEEE International Conference on Mobile Data Management (MDM 2022)* (pp. 385-387). IEEE. <https://doi.org/10.1109/MDM55031.2022.00086>

**Important note**

To cite this publication, please use the final published version (if applicable).  
Please check the document version above.

**Copyright**

Other than for strictly personal use, it is not permitted to download, forward or distribute the text or part of it, without the consent of the author(s) and/or copyright holder(s), unless the work is under an open content license such as Creative Commons.

**Takedown policy**

Please contact us and provide details if you believe this document breaches copyrights.  
We will remove access to the work immediately and investigate your claim.

***Green Open Access added to TU Delft Institutional Repository***

***'You share, we take care!' - Taverne project***

**<https://www.openaccess.nl/en/you-share-we-take-care>**

Otherwise as indicated in the copyright section: the publisher is the copyright holder of this work and the author uses the Dutch legislation to make this work public.

# A framework for indoor localization using the magnetic field

Manon Kok, Frida Viset and Mostafa Osman

Delft Center for Systems and Control, Delft University of Technology, Delft, the Netherlands

Email: {m.kok-1, f.m.viset, m.e.a.osman}@tudelft.nl

**Abstract**—In this work, our focus is on indoor localization using the indoor magnetic field as a source of position information. This relies on the fact that ferromagnetic materials inside buildings cause the magnetic field to vary spatially. We jointly estimate the pose of a combined sensor module (containing a magnetometer) as well as the magnetic field map. We show that our previously developed algorithm for magnetic field-based simultaneous localization and mapping can be adapted and extended into a general framework where a multitude of measurements can be included. We exemplify this using a foot-mounted inertial measurement unit where we additionally assume the availability of range measurements.

**Index Terms**—Indoor localization, magnetic field, SLAM, inertial sensors.

## I. INTRODUCTION

Indoor localization is an active research area because GPS signals get significantly weakened inside buildings [1]. In recent years, the indoor magnetic field has been proposed as a source of position information for indoor localization [2]–[7]. This relies on the fact that ferromagnetic materials inside buildings cause the magnetic field to vary spatially, see also Fig. 1. These spatial variations are known to be largely constant over time [8]. A map of these spatial variations can therefore be used as a source of position information. In recent years, we have developed algorithms for magnetic field-based simultaneous localization and mapping (SLAM) [2]–[5], where we jointly estimate the location of a mobile sensor and a map of the magnetic field in the environment. In this work, we show that it is possible to extend the idea of SLAM using the magnetic field to a general framework where we estimate the sensor pose using odometry in combination with various types of measurements that complement the position information from the magnetic field. We exemplify this using a foot-mounted inertial measurement unit (IMU) where we, apart from the magnetic field, also use range measurements to improve the pose estimation.

## II. FRAMEWORK FOR INDOOR LOCALIZATION USING THE MAGNETIC FIELD

We are interested in jointly estimating  $x_t := [(x_t^p)^T \ m^T]^T \in X$ , where  $m$  denotes a stationary magnetic field map and  $x_t^p := [(p_t^n)^T \ (q_t^{ns})^T]^T$  denotes the time-varying states. Here,  $p_t^n$  is the sensor's position and  $q_t^{ns}$  its orientation. The superscript “n” explicitly indicates that we express this position and velocity in a world-fixed navigation frame, while the superscript “s” refers to a sensor-fixed frame.

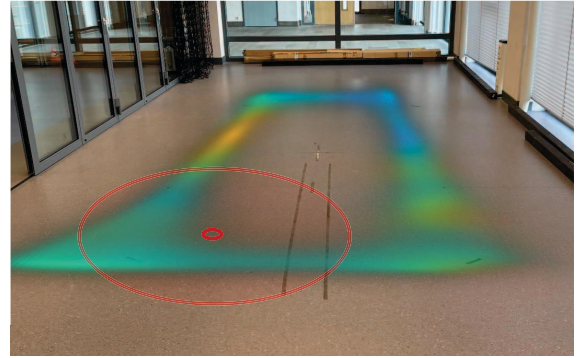


Fig. 1. The estimated magnetic field for an experimental sequence collected in an optical motion capture lab. In addition to the collected inertial and magnetometer data, we simulate range measurements with respect to a stationary beacon (small red circle) with a finite range visualized by the large red circle.

We parametrize the orientation using a unit quaternion and denote the rotation matrix representation of this orientation by  $R_t^{ns}$  and the reverse rotation by  $R_t^{sn}$ . Note that  $x_t^p$  can also include further states such as the sensor's velocity or sensor biases. We assume a calibrated combined sensor module and model the change in  $x_t^p$  as

$$x_t^p = f(x_{t-1}^p, u_t) + w_t, \quad (1)$$

where  $u_t \in U$  is an input vector,  $f : X \times U \rightarrow X$  and  $w_t \sim \mathcal{N}(0, Q)$  is white process noise.

We model the magnetic field map as a Gaussian process (GP). GP regression scales cubically with the number of data points. Because of this, we use a reduced-rank approximation to the GP [9] in the same way as in [5]. This approximation models the GP in terms of a number of basis functions on a fixed domain, assuming that the magnetic field anomalies are zero at the boundary. This has been shown to be a good approximation if sufficiently many basis functions and a large enough domain are used [9]. Hence, the three-dimensional magnetometer measurements  $y_{m,t}$  are modeled as

$$y_{m,t} = R_t^{sn} C(p_t^n) m + e_{m,t}, \quad e_{m,t} \sim \mathcal{N}(0, \sigma_m^2 I_3), \quad (2)$$

where  $C(p_t^n) \in \mathbb{R}^{3 \times m_b}$ , with  $m_b$  the number of basis functions, depends nonlinearly on the position  $p_t^n$ . Furthermore,  $e_{m,t}$  is white measurement noise. For more details, see [5].

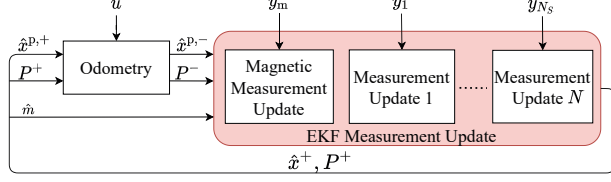


Fig. 2. Overview of the proposed framework for indoor localization using the magnetic field.

The framework allows for including any other measurements that are available. The available sensors in the module are modeled as

$$y_{i,t} = h_i(x_t) + e_{i,t}, \quad \forall i = 1, \dots, N_S, \quad (3)$$

where  $y_{i,t} \in Y_i$  is the measurement received from the  $i$ -th sensor in the sensor module,  $h_i : X \rightarrow Y_i$  is the (nonlinear) measurement model of the  $i$ -th sensor,  $e_{i,t} \sim \mathcal{N}(0, \mathcal{R}_i)$  is white measurement noise, and  $N_S$  is the number of sensors present in the module in addition to the magnetometer.

The framework uses an extended Kalman filter (EKF) to estimate the states  $x_t$  by using the magnetometer measurements along with the other heterogeneous sensors present in the combined sensor module. The EKF uses the odometry to obtain a prediction  $\hat{x}_t^{p,-}$ . It also updates the covariance of the state estimates  $\hat{x}_t^{p,-}$  in the state covariance matrix  $P_t^-$ . It then uses the magnetometer and additional sensor measurements to obtain a posterior mean  $\hat{x}_t^+$  and covariance  $P_t^+$ . Note that the magnetometer measurements provide information both about  $x_t^p$  and the map  $m$ , see (2). Hence, no explicit fingerprinting is necessary. Slightly deviating from a standard EKF implementation, we do not update the cross covariance between  $\hat{x}_t^{p,-}$  and  $m$  in  $P_t^-$  in the EKF prediction. This results in a considerable speed-up of the algorithm and makes it more robust against unmodeled errors in the odometry. An overview of the proposed framework is shown in Fig. 2.

### III. CASE STUDY

To illustrate the proposed framework for indoor localization using the magnetic field, we apply it to the problem of localizing a foot-mounted IMU using magnetometer measurements in combination with simulated range measurements.

#### A. Odometry

We use a standard dynamic model [10] where the accelerometer measurements  $y_{a,t}$  and the gyroscope measurements  $y_{\omega,t}$  are used as inputs  $u_t$  to the model (1). In other words, the dynamic model does not make any explicit assumption about the motion of the sensor but rather models the change in position, velocity and orientation to correspond to the measured acceleration and angular velocity. More specifically,

$$\begin{bmatrix} p_{t+1}^n \\ v_{t+1}^n \\ q_{t+1}^{ns} \end{bmatrix} = \begin{bmatrix} p_t^n + T v_t^n + \frac{T^2}{2} (R_t^{ns} y_{a,t} + g^n - e_{a,t}) \\ v_t^n + T (R_t^{ns} y_{a,t} + g^n - e_{a,t}) \\ q_t^{ns} \odot \exp_q \left( \frac{T}{2} (y_{\omega,t} - e_{\omega,t}) \right) \end{bmatrix}, \quad (4)$$

#### Algorithm 1 Inertial sensor-based foot-mounted indoor localization using the magnetic field

**Input:** Accelerometer, gyroscope and magnetometer measurements  $\{y_{a,t}, y_{\omega,t}, y_{m,t}\}_{t=1}^{N_T}$  and additional available measurements  $\{y_{r,t}\}_{t=1}^{N_T}$ .

**Output:** Estimated position, velocity, orientation and magnetic field map  $\hat{x}_t^+$  for  $t = 1, \dots, N_T$ .

- 1: Initialize the state  $\hat{x}_0^+$ .
- 2: **for**  $t = 1$  to  $N_T$  **do**
- 3:   **Odometry:** Update  $\hat{x}_{t-1}^{p,+}, P_{t-1}^{p,+}$  to  $\hat{x}_t^{p,-}, P_t^{p,-}$  using the dynamic model (4), the inertial measurements, the zero velocity and zero height updates.
- 4:   **Measurement update:** Compute  $\hat{x}_t^+, P_t^+$ :
- 5:     If magnetometer measurements are available, update the state estimate and its covariance using (2).
- 6:     If range measurements are available, for each beacon  $i$ , update the state estimate and its covariance using (5).
- 7: **end for**

where  $g^n$  denotes the Earth's gravity,  $T$  the sampling time and  $e_{a,t} \sim \mathcal{N}(0, \sigma_a^2 \mathcal{I}_3)$ ,  $e_{\omega,t} \sim \mathcal{N}(0, \sigma_\omega^2 \mathcal{I}_3)$ . Furthermore,  $\odot$  denotes the quaternion multiplication and  $\exp_q$  converts a 3-dimensional vector to a unit quaternion [10].

Moreover, we exploit the fact that the IMU is foot-mounted to enhance the accuracy of the odometry by using zero velocity and zero height updates. The foot steps are detected in the same way as in [11].

#### B. Measurement model

In addition to the magnetic field measurement model (2), we assume that range measurements  $y_{r,t}$  with respect to a beacon at a fixed position  $p_b^n$  are available which can be modeled as

$$y_{r,t} = \|p_t^n - p_b^n\|_2 + e_{r,t}, \quad e_{r,t} \sim \mathcal{N}(0, \sigma_r^2). \quad (5)$$

#### C. Methods

Similar to the approach in [5] we use an EKF with error states and relinearize the state for each measurement update. We initialize the magnetic field map based on the GP prior, for more information see [5]. This initialization relies on knowledge of a number of hyperparameters. As is common in existing methods, we assume that these hyperparameters are known and fixed.

### IV. RESULTS

We evaluate the workings of Algorithm 1 using data collected with a foot-mounted IMU (Xsens MTi-100).<sup>1</sup> Ground truth data was collected using an optical motion capture system (Optitrack). The experimental setup is shown in Fig. 3. We simultaneously collected inertial measurements at 200 Hz and use magnetometer measurements at 2 Hz. Range measurements were simulated from a beacon placed at the

<sup>1</sup>Our Matlab implementation producing the results can be found on <https://github.com/fridaviset/MagSLAM-Framework>.

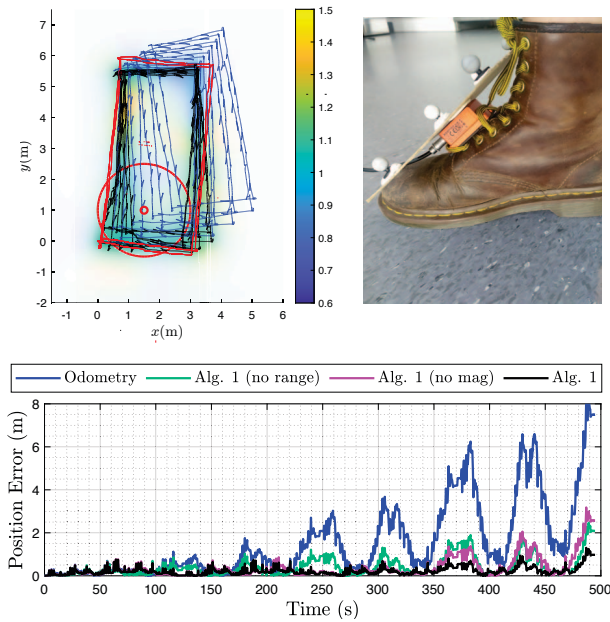


Fig. 3. The experimental setup (top right) and the estimated path by the proposed framework with the captured ground-truth (top left) and the translation errors of the different algorithms (bottom). The collected ground-truth data is shown in red, the odometry is shown in blue, and the output of Alg. 1 is shown in black. Additionally, the simulated beacon and its range are shown as red circles in the top left plot.

location shown in Fig. 3. We assume that the beacon has a range of 1.5 m, visualized as the red circle, that the range measurements are available every 20 samples, corresponding to a sampling time of 10 Hz, and that  $\sigma_r^2 = 0.1$ . We collected two square laps of data but to better illustrate the workings of our algorithm, we extend the data set by repeating it four times. We use the same hyperparameters as in [3] for the magnetic field map. Furthermore, we assumed that the range measurements were only available for the first 200 seconds.

In Fig. 3 it can be seen that while the odometry drifts, resulting in a position RMSE of 2.36 m, the RMSE of Algorithm 1 is 0.27 m. The estimated magnetic field map is visualized in Fig. 3 but can be seen more clearly in Fig. 1. In both figures, we visualize the norm of the magnetic field while the opacity is inversely proportional to the uncertainty of the GP map posterior.

We compare the estimation accuracy of Algorithm 1 with using the algorithm either without magnetometer measurements or without range measurements. This results in RMSEs of 0.60 m and 0.61 m, respectively. The results shows the efficacy of the proposed framework in solving the indoor localization problem. Additionally, it shows that by including the combination of magnetometer with another type of measurements (range measurements), the accuracy of the localization output is improved.

## V. CONCLUSIONS

We presented a framework for indoor localization using the magnetic field and illustrated its efficacy using a foot-mounted

IMU and assuming the availability of range measurements. One of the challenges in practice is the computational complexity of constructing the magnetic field map and we plan to address this in future work. For instance, the hexagonal maps from [2] can be used to make the approach scalable to larger domains. We are also interested in exploring different types of additional sensors to use in the framework or to replace the inertial measurements with wheel odometry from a mobile robot. Note that the method does not work if there is insufficient information about the pose in the measurements. An interesting direction of future work is therefore also to explore the minimum amount of information that is needed for magnetic field SLAM or reversely, how sensors can be combined to result in a robust solution for indoor localization.

## ACKNOWLEDGMENT

This publication is part of the project “Sensor Fusion For Indoor Localisation Using The Magnetic Field” with project number 18213 of the research program Veni which is (partly) financed by the Dutch Research Council (NWO).

## REFERENCES

- [1] S. Adler, S. Schmitt, K. Wolter, and M. Kyas, “A survey of experimental evaluation in indoor localization research,” in *Proceedings of the IEEE International Conference on Indoor Positioning and Indoor Navigation (IPIN)*, Banff, Alberta, Canada, Oct. 2015, pp. 1–10.
- [2] M. Kok and A. Solin, “Scalable magnetic field SLAM in 3D using Gaussian process maps,” in *Proceedings of the 20th International Conference on Information Fusion*, Cambridge, UK, July 2018, pp. 1353–1360.
- [3] M. Osman, F. Viset, and M. Kok, “Indoor slam using a foot-mounted IMU and the local magnetic field,” *ArXiv e-prints*, Mar. 2022, arXiv:2203.15866.
- [4] F. Viset, J. T. Gravdahl, and M. Kok, “Magnetic field norm SLAM using Gaussian process regression in foot-mounted sensors,” in *Proceedings of the European Control Conference (ECC)*, Rotterdam, the Netherlands, Jun. 2021.
- [5] F. Viset, R. Helmons, and M. Kok, “An extended Kalman filter for magnetic field SLAM,” *MDPI Sensors (accepted for publication)*, 2022. [Online]. Available: [tinyurl.com/kbxywpyy](https://tinyurl.com/kbxywpyy)
- [6] I. Vallivaara, J. Haverinen, A. Kemppainen, and J. Rönning, “Simultaneous localization and mapping using ambient magnetic field,” in *Proceedings of the IEEE Conference on Multisensor Fusion and Integration for Intelligent Systems (MFI)*, Salt Lake City, UT, USA, September 2010, pp. 14–19.
- [7] M. Angermann, M. Frassl, M. Doniec, B. J. Julian, and P. Robertson, “Characterization of the indoor magnetic field for applications in localization and mapping,” in *Proceedings of the International Conference on Indoor Positioning and Indoor Navigation (IPIN)*, Sydney, Australia, 2012, pp. 1–9.
- [8] B. Li, T. Gallagher, A. G. Dempster, and C. Rizos, “How feasible is the use of magnetic field alone for indoor positioning?” in *Proceedings of the International Conference on Indoor Positioning and Indoor Navigation (IPIN)*, Sydney, Australia, Nov. 2012, pp. 1–9.
- [9] A. Solin and S. Särkkä, “Hilbert space methods for reduced-rank Gaussian process regression,” *Statistics and Computing*, vol. 30, pp. 419–446, Mar. 2020.
- [10] M. Kok, J. D. Hol, and T. B. Schön, “Using inertial sensors for position and orientation estimation,” *Foundations and Trends on Signal Processing*, vol. 11, no. 1–2, pp. 1–153, 2017.
- [11] J. Nilsson, I. Skog, P. Händel, and K. V. S. Hari, “Foot-mounted INS for everybody - an open-source embedded implementation,” in *Proceedings of the IEEE/ION Position, Location and Navigation Symposium*, Myrtle Beach, SC, USA, April 2012, pp. 140–145.